Phonons as a probe of short-range order in $Si_{1-x}C_x$ alloys

H. Rücker, M. Methfessel, B. Dietrich, K. Pressel, and H. J. Osten
Institut für Halbleiterphysik, P.O. Box 409, D-15204 Frankfurt (Oder), Germany
(Received 2 August 1995)

This paper shows that by combining theoretical and experimental results for local Si-C phonon modes in dilute $Si_{1-x}C_x$ alloys, information concerning the short-range order can be obtained. Calculations using an anharmonic Keating model predict satellite peaks near the vibrational frequency of an isolated C impurity which are associated with second-, third-, etc., nearest-neighbor C-C pairs. By comparing theoretical spectra with those obtained by Raman and infrared absorption spectroscopy, we conclude that the probability for a third-nearest-neighbor coordination of the C atoms is considerably above that for a purely random alloy. This confirms earlier work predicting an attractive third-nearest-neighbor interaction of the C impurities due to elastic interactions.

I. INTRODUCTION

In substitutional alloys, one of the more interesting questions is whether the atoms are arranged according to some short-range order. This important information is generally difficult to obtain experimentally. In covalent materials the interatomic forces are dominated by short-range interactions so that the lattice vibrations probe the local atomic geometry. By combining theoretical predictions with the measurement of Raman and infrared absorption spectra, we show here how information on the local order can be obtained from the satellite structure of the phonon modes for dilute silicon-carbon alloys.

We focus on $Si_{1-x}C_x$ alloys, which are candidates as possible materials for the fabrication of Si-based heterostructures.[1–3] Using improved growth techniques, defect-free pseudomorphic epitaxial layers of $Si_{1-x}C_x$ as well as similar ternary alloys containing Ge with a small amount of carbon ($0 \leqslant x \leqslant 0.02$) can be grown (see Ref. 4 for a review). The phonons in Si-C alloys have been studied previously using Raman[5–7] and infrared absorption spectroscopy[3] without consideration of the fine structure.

A central feature of a dilute $Si_{1-x}C_x$ alloy is that the carbon atoms mainly occupy substitutional lattice sites. This is supported, for example, by the approximate validity of Vegard's rule for this system and by resonant Rutherford backscattering experiments.[9] Although substitutional alloying is the expected behavior for alloys such as $Si_{1-x}Ge_x$ in which the constituents have similar sizes, it is not at all obvious for $Si_{1-x}C_x$. The equilibrium volume of carbon is about 70% smaller than that of Si so that a substitutional C impurity is accompanied by an energetically costly strain field. Thus, we are confronted by the interesting situation that the C atoms do not really ''fit into the lattice'' but are nevertheless held there by the strong directional covalent bonding. In fact, although the substitutional position has the lowest energy for an isolated C impurity, several C atoms can cooperate to avoid the elastic strain by combining to make complexes.[10,11]

One direct consequence of the tension between the size discrepancy and the directed bonding forces is a prominent oscillatory structure[12] in the pair interaction between two substitutional carbon impurities. Specifically, a C-C pair is *bound* by about 0.14 eV at the third-nearest-neighbor (3nn) distance. For other arrangements such as first-, second-, and fifth-nearest neighbors, the interaction is repulsive. These energies are a simple consequence of the local geometry. The energy gain at the 3nn distance arises because the C atoms lie at opposite positions in a sixfold ring, which can relax to accommodate the short Si-C bond with minimal bond-bending distortions. Repulsive interactions result when the two C atoms lie in the same zigzag chain in the (110) direction because strain is easily transmitted along these.

It turns out that the C-C interaction energy strongly influences the local vibrational modes in a Si-C alloy, which we have calculated here using a recently developed anharmonic variant[13] of Keating's valence force model,[14] applied to large supercells with random occupations of the sites. This procedure predicts a fine structure near the Si-C peak which can be used to identify specific configurations in a measured Raman or infrared spectrum. The shift of the satellite peak relative to the frequency of the isolated impurity is directly related to the oscillatory pair interaction. A C-C arrangement is energetically favorable for those cases in which the Si-C bond can relax to a larger extent towards its native short value. This leads to a stiffening of the bonds and higher vibrational frequencies. Conversely, an unfavorable arrangement is associated with more strongly stretched bonds and lower frequencies.

Using Raman and infrared spectroscopy on $Si_{1-x}C_x$ samples made by molecular-beam epitaxy (MBE), we were able to observe the 3nn satellite peak at the predicted position. A detailed comparison of the measured and calculated spectra shows that the C atoms are not distributed at random. Instead, we conclude a substantial enhancement of the third-nearest-neighbor C-C coordination in agreement with the predicted attractive interaction at this distance.

The rest of this paper is organized as follows. In Sec. II we present the microscopic theory based on the anharmonic Keating model used to calculate the relaxed geometry and phonon frequencies in the $Si_{1-x}C_x$ alloys. The experimental procedure and results are presented in Sec. III. A detailed comparison of the measured and calculated Raman and infrared absorption spectra is used in Sec. IV to extract information on the short-range order. The results are summarized in Sec. V.

TABLE I. Force constants α and β and equilibrium lattice constants a_0 in atomic units used in the calculations.

	a_0	α	β
C	6.68	0.137	0.101
Si	10.21	0.058	0.017
SiC	8.17	0.088	0.036

II. THEORY

A. Anharmonic Keating model

Substitutional alloys of Si and C exhibit large local strain due to the large difference in the size of Si and C atoms. Deformations of individual bonds in the alloy are far beyond those that are realized in crystals under external pressure. As a consequence, the strain energy is no longer a quadratic form in the deformations and anharmonic terms should be included. In order to include these effect we have recently developed an anharmonic variant[13] of the well-known Keating model,[14] designed for semiconductor alloys containing atoms with large size differences.

In the standard Keating model the strain energy W is taken to depend on the vectors $\mathbf{r}_{ij}$ connecting nearest-neighbor lattice sites i and j as follows:

$$W=\sum_{i,j}\frac{\alpha}{a_0^2}[\Delta(r_{ij}^2)]^2+\sum_{i,j,k\neq j}\frac{\beta}{a_0^2}[\Delta(\mathbf{r}_{ij}\cdot\mathbf{r}_{ik})]^2, \qquad (1)$$

where Δ denotes the change relative to the perfect lattice due to a distortion, i.e., $\Delta(\mathbf{r}_{ij}\cdot\mathbf{r}_{ik})=\mathbf{r}_{ij}\cdot\mathbf{r}_{ik}-\mathbf{r}_{ij}^0\cdot\mathbf{r}_{ik}^0$ is the change of the scalar product between the two vectors connecting atom i with its neighbors j and k. Based on *ab initio* density-functional calculations we have determined a suitable explicit dependence of the bond-stretching (α) and bond-bending (β) force constants on the local geometry. It was found that the volume dependence of the elastic properties from the *ab initio* calculations is well reproduced over a very large range when certain universal scaling laws for the force constants with the bond lengths are adopted. Namely, the force constants α and β scale with the fourth and the seventh power of the inverse bond length, respectively. The Si-C alloy is characterized by the different force constants describing the pure Si, C, and β-SiC crystals (whereby the C force constants do not enter for structures without nearest-neighbor C-C pairs). The parameters used in the calculations below and listed in Table I were determined in Ref. 13 from a least-squares fit to elastic constants and the zone-center optical phonons of Si, diamond, and β-SiC. By including the scalings, the anharmonic model gives the same elastic constants and phonon frequencies as the standard model at the equilibrium volume but the useful range is extended to much larger distortions. In this way the large bond-stretching distortions (typically by 8% for the Si-C bond) in the substitutional $Si_{1-x}C_x$ alloys are described properly.

B. Pair interaction of substitutional C atoms

Substitutional C impurities in a silicon lattice can interact via their strain fields. The interaction energy of a pair of substitutional C atoms is defined as the energy of the C-C pair at a given distance minus twice the energy of an isolated C impurity. To obtain the interaction energy using the anharmonic Keating model we have first calculated the strain energy W for a single substitutional C atom in Si. The system was described by a periodic supercell of 2000 atoms whereby one Si atom was substituted by a C atom. The positions of the atoms were relaxed until all forces vanished. In the next step a similar calculation was done with carbon atoms substituted for two sites of the supercell. By repeating this procedure for carbon atoms at various relative positions we obtain the interaction energies as a function of the C-C distance as shown in Fig. 1.

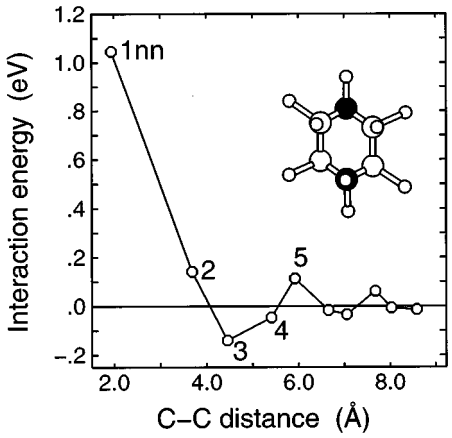

FIG. 1. Interaction energy of two substitutional carbon atoms in silicon as calculated from the anharmonic Keating model. Circles indicate the energies for pairs of C atoms relative to the energy of two isolated substitutional C impurities. Coordinations ranging up to the tenth-nearest-neighbor distance were considered. The line is to guide the eye. The inset shows the third-nearest-neighbor arrangement of two carbon atoms (black).

An unexpected result is that the interaction of two C impurities shows negative as well as positive values, that is, that the carbon pair is bound at certain distances. This effect is purely elastic in origin. For example, the attractive interaction for C atoms arranged as third-nearest neighbors comes about because the C atoms lie at opposite corners of a sixfold ring (inset in Fig. 1). For this geometry the short Si-C bonds can be accommodated relatively easily without strong bond-bending distortions. Similarly, the repulsive 2nn, 5nn, and 8nn interactions arise because the C atoms lie in the same relatively rigid zigzag (110) chain.

The carbon pair is most strongly bound (by the respectable value of 0.14 eV) at the third-nearest-neighbor coordination. For carbon-rich samples this was shown to lead to a tendency to order into phases that have many third-nearest-neighbor carbon pairs.[12] In the present paper we show that the bound carbon pair can be detected in the phonon spectrum of a dilute disordered $Si_{1-x}C_x$, alloy, thereby supplying information about the short-range order.

C. Calculation of phonon spectra

The lattice dynamical properties of a crystal are described by its dynamical matrix containing the second derivatives of the total energy with respect to the atomic displacements.

Using the Keating model, the matrix can easily be built up directly and diagonalized using standard routines, even for large supercells that simulate an alloy. We have used 512-atom supercells with a random distribution of the atoms over the lattice sites according to the stoichiometry. Because of the very strong repulsion for nearest-neighbor carbon atoms, only configurations without such pairs were considered. To reduce statistical fluctuations, the calculated spectra were averaged over 40 random configurations. To simulate pseudomorphic growth on a Si substrate, the lattice constants in x and y directions were fixed at the corresponding value but the supercell was permitted to relax vertically.

Both Raman and infrared spectra can be determined from the eigenstates. This is mainly a matter of including appropriate selection rules and a simple treatment is adequate. To obtain Raman spectra, we follow the procedure given in Ref. 15. Assuming the same polarizability for all atoms, the off-resonance Raman intensity is given, up to a multiplicative constant, by

$$\sigma^{\alpha\beta} \propto \sum_{\nu} \frac{2\Gamma\omega}{(\omega_{\nu}^2-\omega^2)^2+\Gamma^2\omega^2}\left|\sum_i s_i u_{i\gamma}^{\nu}\right|^2, \qquad (2)$$

where ν runs over all phonon modes, $\mathbf{u}_i^{\nu}$ is the displacement vector of the atom at lattice site i, and s_i is, respectively, $+1$ and -1 for the two fcc sublattices of the diamond structure. The Cartesian indices α, β, and γ specify the polarization and a Lorentzian line shape with a broadening Γ is assumed.

Infrared absorption by a Si-C compound is possible because of charge transfer from the Si to C atoms, leading to a lattice of non-neutral ions. This effect can be most directly treated within a rigid-ion model.[16] To specify the ion charge for a site in the disordered alloy, we assume that all Si-C bonds have the same polarity and count the Si and C nearest neighbors. In our geometries each C atom is surrounded by four Si atoms and thus has the same charge $z_C^*=z^*$. A Si atom can have from zero to four C neighbors, giving a charge z_{Si}^* equal to $-1/4z^*$ times this number. For cubic SiC, the rigid-ion model predicts the splitting of the TO and LO modes at Γ, which can be used to fix the effective (dynamical) charge z^*. The absorption coefficient for infrared light is given by the imaginary part ϵ_2 of the dielectric function. Again using Lorentzian broadening, ϵ_2 can be expressed using the eigenvectors $\mathbf{u}_i^{\nu}$ of the atomic displacement as follows:

$$\epsilon_2^{\alpha\beta} \propto \sum_{\nu} \frac{2\Gamma\omega}{(\omega_{\nu}^2-\omega^2)^2+\Gamma^2\omega^2}\sum_{i,j} z_i^* z_j^* u_{i\alpha}^{\nu} u_{j\beta}^{\nu}. \qquad (3)$$

The effective charge z^* enters as an overall multiplicative constant and does not have to be specified for our purposes. It should be mentioned that the charge transfer from Si to C causes long-range electrostatical interactions, which are neglected in the Keating potential but which can be added explicitly in a modified model.[17]

D. Discussion of the Si-C modes

A typical calculated Raman spectrum for a pseudomorphic $Si_{0.99}C_{0.01}$ layer on a Si(001) substrate is shown in Fig. 2. The strong peak at 530 cm^{-1} is due to Si-Si vibrations. Its position is close to the Raman peak in pure Si, which in our model lies at 531 cm^{-1}. The peak due to localized Si-C vibrations lies at 612 cm^{-1}. Experimentally,[18,10] the Si-Si and Si-C frequencies are found at 520 cm^{-1} and 605 cm^{-1}, respectively, so our model (perhaps accidentally) gives extremely good agreement for the separation between these peaks.

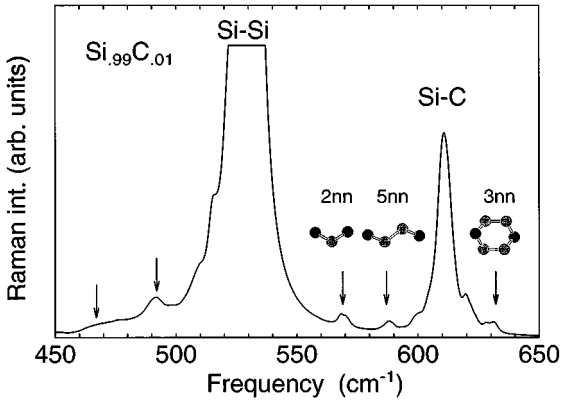

FIG. 2. Calculated Raman spectrum for an epitaxial $Si_{0.99}C_{0.01}$ layer on Si(001). A Lorentzian broadening $\Gamma = 3$ cm^{-1} was assumed. Satellites of the C-Si impurity peak are indicated by arrows and sketches of the associated microscopic arrangements of second-, third-, and fifth-nearest-neighbor C-C pairs. Features marked on the low-energy side of the main Si-Si peak are discussed in Sec. III B.

Our interest focuses on the small but clear satellites near the Si-C peak in Fig. 2. Not unexpectedly, inspection of the phonon eigenvectors shows that these are also Si-C vibrations. We associate the satellites with specific arrangements of carbon pairs as indicated in the figure. To demonstrate this, we have done additional calculations for supercells containing a single carbon atom and for two carbon atoms at various distances. The lower part of Fig. 3 shows the calculated Raman spectra for these cases. For a pair of carbon atoms, the six vibrational modes are arranged in several subpeaks, which can be Raman active, infrared active, both, or neither, depending on the symmetry. Of the Raman-active subpeaks, some typically lie close to the isolated impurity frequency but one can be shifted by a considerable amount, leading to the visible satellites in the alloy spectrum. This is confirmed by the comparison to the alloy spectrum of Fig. 2, redrawn at the top of Fig. 3 for convenience.

In a more detailed manner, we can assemble the alloy spectrum from the spectra of the C impurity and the different C-C pairs by a suitable weighting procedure. If x is the carbon concentration, y is defined as $1-x$, and N_n is the number of sites in the nth shell around a selected site, then $q_n=y^{N_n}$ is the probability that no carbon atoms are found in this shell. Consequently $s_n=q_1q_2\cdots q_n$ is the probability that no carbon atom lies in shells 1 through n. Since $r_n=1-q_n$ is the probability that at least one carbon atom is in the nth shell, the relevant quantity is

$$w_n=r_n s_{n-1}=(1-y^{N_n})y^{N_1+\cdots+N_{n-1}}. \qquad (4)$$

This is the probability that the closest carbon neighbor lies in the n-th shell. Each w_n is used as the weight factor for the Raman spectrum of the associated C-C pair, where we have

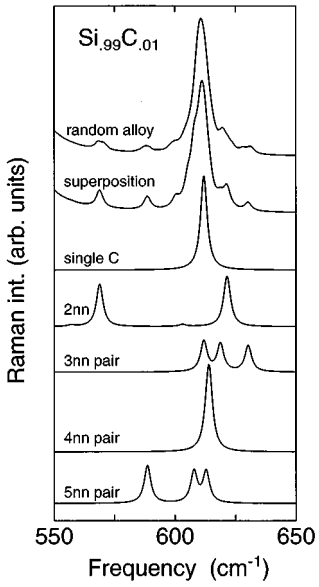

FIG. 3. Top: calculated Raman spectrum for a Si-C alloy containing 1% carbon, as obtained using simulations with 512-atom supercells and a random occupation of the lattice sites. Second curve: the spectrum for the same alloy, obtained by a suitable weighted sum of the spectra for C-C pairs arranged as second-, third-, etc., nearest neighbors and the isolated C impurity. The partial spectra for these configurations are shown in the lower part of the figure.

included terms up to $n=22$. The weight factor w_1 was set to zero in order to prohibit strongly repulsive nearest-neighbor C-C pairs. Finally, the spectrum of the isolated C impurity is given a weight

$$w_0 = 1 - \sum_i w_i . \tag{5}$$

The spectrum assembled in this way is displayed as the second curve in Fig. 3, showing that the relative heights of the peaks are reasonably well reproduced by the weighting procedure. Note that in calculating the weight w_n, we have not considered whether the closest carbon atom to the selected carbon site has itself other carbon neighbors that are closer than nth-nearest neighbor. This definition of w_n, while at first sight incorrect, is appropriate in view of the discussion in the next paragraph.

We consider it a central result that the vibrational frequencies of the substitutional C-C pairs at different coordinations (Fig. 3) are directly related to the C-C binding curve (Fig. 1) which was discussed in Sec. II B. It was noted above that one of the Raman-active peaks generally lies either significantly above or below the frequency of the isolated C impurity. (This discussion proceeds in the same way if the infrared modes or the total phonon density of states is considered.) The distribution of the frequencies is contrary to the experience that an interaction generally splits the peaks in a manner that maintains their average value. To understand the situation here, consider the third-nearest-neighbor configuration, which is bound by about 0.14 eV. The binding energy is mainly due to the fact that some of the short Si-C bonds are less strongly stretched in this configuration than around an isolated impurity. Consequently these bonds are stiffer, as is described by Grüneisen's parameter, producing vibrational modes at a higher frequency. Conversely, pair configurations with a repulsive interaction are associated with longer Si-C bonds, reduced bond stiffness, and lower vibrational frequencies. Inspecting Fig. 3 from this viewpoint shows clearly that the position of the splitoff Raman peak closely follows the binding energy of the corresponding C-C pair.

Due to the mass difference, the Si neighbors of a carbon atom hardly participate in vibrations with a large amplitude on the C site. The vibrating system thus consists essentially of a single carbon impurity in an unsymmetric environment. This environment is mainly determined by the position of the closest carbon neighbor, as was anticipated in the calculation of the weights w_n. The direct vibrational interaction of the two carbon atoms is much less important. In a systematic manner, those pair configurations that are bound relative to the isolated impurities lead to peaks shifted to higher energies, and vice versa.

III. EXPERIMENT

A. Sample preparation

The layers were grown in a solid-source molecular-beam epitaxy apparatus using a pyrolytic graphite-filament sublimation cell as a solid carbon source. The growth procedure is described in detail in Ref. 8. The size of the samples was 18 mm $\times$ 25 mm. During growth one part of the sample with a size of approximately 4 mm $\times$ 4 mm was covered by the sample holder and thus could be used as reference piece for the Raman and absorption measurements. The carbon concentrations were monitored by x-ray diffraction and secondary-ion-mass spectroscopy.

B. Raman spectroscopy

The Raman measurements were performed with a Dilor "xy" micro-Raman spectrometer. The spectrometer was equipped with three identical 1800 grooves/mm gratings that had a focal length of 500 mm. The first two gratings were used in subtractive arrangement as a double monochromator. Thus a spectral resolution of 3.2 cm^{-1} was achieved. In special cases a triple additive arrangement was used yielding a spectral resolution of 1.1 cm^{-1}. The samples were excited through a confocal optical system with the 514.5-nm line of an Ar^+-ion laser and a power of 20 mW. A microscope objective with a 0.95 numerical aperture collected the scattered intensity. After passing the spectrometer, the inelastically scattered light was detected by a cooled charge-coupled device matrix. The Raman spectra were investigated in backscattering $z(x,y)\bar{z}$ geometry.

The contribution due to the carbon vibrational mode to the total Raman signal is expected to be small for the considered carbon concentrations less than 1% and layer thicknesses of about 100 nm, which is only 1/10 of the penetration depth of the laser light in silicon. If we assume that the Raman scattering efficiency of the carbon related local vibrational modes in the alloy is similar to the scattering efficiency of the Si-Si vibrations it can be estimated that the carbon-related signal is only 1/1000 of the intensity of the

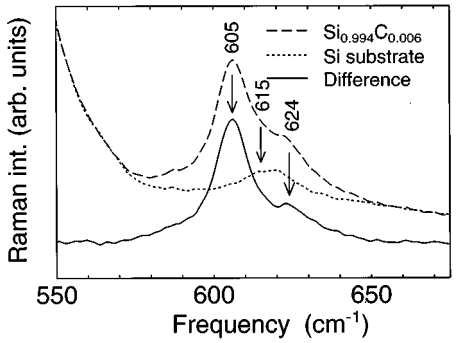

FIG. 4. Raman spectra of the $Si_{0.994}C_{0.006}$/Si(001) heterostructure and the Si substrate taken under identical experimental conditions. The lower curve is the difference between the two spectra and gives the contribution from the pseudomorphic silicon-carbon alloy layer.

Si-Si vibrational mode. Thus, it is important to distinguish carefully between the contributions of the $Si_{1-x}C_x$ layer and the silicon substrate.

The separation of the $Si_{1-x}C_x$ and Si signals is complicated since the Raman spectrum of the Si substrate is not smooth in the interesting region of the local vibrational modes of carbon but shows a weak peak near 615 cm^{-1}. This peak is due to a combination of one acoustical and one optical phonon. While the selection rules for the employed scattering geometry prohibit two-phonon overtones, the peak near 615 cm^{-1} is the only two-phonon combination observed in bulk silicon.[19]

To separate the carbon contribution to the measured Raman signal a silicon spectrum was subtracted from the total spectrum as demonstrated in Fig. 4. The upper two spectra are measured spectra from a sample region covered with the pseudomorphic $Si_{0.994}C_{0.006}$ layer and from the uncovered Si-substrate region in the corner of the sample. Both spectra were measured successively under identical experimental conditions for equal measuring periods in triple additive arrangement. They were normalized to the peak intensity of the Si-Si mode before the Si spectrum was subtracted. The resulting difference is shown in the lower curve of Fig. 4. The difference spectrum shows the well-known peak of local vibrational modes of carbon at 605 cm^{-1}. Additionally, a satellite peak near 625 cm^{-1} was resolved in this and a series of similar $Si_{1-x}C_x$ samples. It is clearly seen that the peaks we identify as carbon-related are not artifacts due to the substrate. Furthermore, note that the half widths of the localized carbon modes are smaller than those of the two-phonon peak from the substrate.

We exclude the possibility that the observed satellite peak near 625 cm^{-1} is caused by localized boron vibrations. To prove this we have measured the Raman spectrum for a pure Si layer deposited by MBE on a Si substrate under the same conditions. Although the process-induced boron contamination can be assumed to be the same as for the $Si_{1-x}C_x$ epilayer the peak near 625 cm^{-1} was not observed for the pure Si epilayer.

We point out that the Raman measurement shows shoulders at 470 cm^{-1} and 495 cm^{-1} to the low-energy side of the Si-Si phonon mode. These are reproduced in our calculation (Fig. 2). From the calculations, we could determine that these are Si-Si modes and that they are related to the softening of the stretched Si-Si bonds near the C impurity. A shoulder near 470 cm^{-1} was also seen by Tsang *et al.*[5]

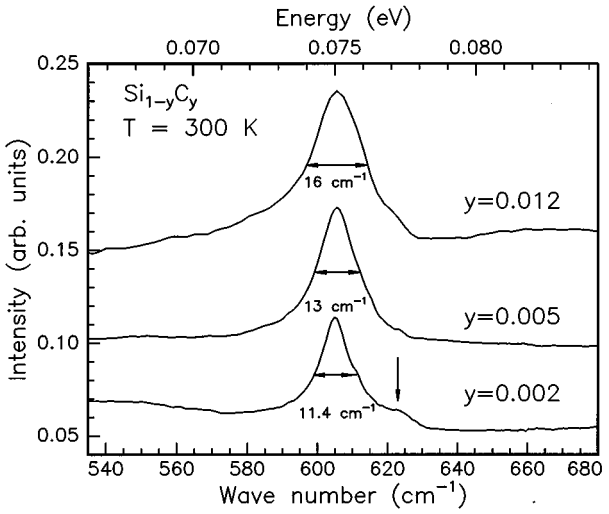

FIG. 5. Infrared absorption spectra of the vibrational mode of substitutional carbon in three different SiC samples with carbon concentrations 0.2%, 0.5%, and 1.2%.

C. Infrared absorption spectroscopy

The infrared-absorption measurements in the optical region at about 600 cm^{-1} were performed with a BOMEM DA8.02 Fourier-transform spectrometer, which was evacuated during the measurements. The light source was a globar, which was warmed up for more than 1 h to gain stability. A KBR beam splitter was used for detection. The light was detected with a Si bolometer. In the range of the vibrational mode of substitutional carbon the silicon substrate has strong multiphonon absorptions. Thus, differential spectra are required. To obtain the spectra of the $Si_{1-x}C_x$ layer we have subtracted the absorption spectrum of the substrate part of the sample, which was not covered with a $Si_{1-x}C_x$ layer during growth, from the absorption spectrum of the $Si_{1-x}C_x$ layer with the substrate. To check the stability of the apparatus all the measurement were repeated several times. For example, the absorption spectrum of the substrate with the $Si_{1-x}C_x$ pseudomorphic layer was registered several times for more than 1 h and then the spectra were divided by each other. The apparatus was assumed to be stable when the result of this division was a straight line.

Figure 5 shows absorption spectra of three different $Si_{1-x}C_x$ strained layers grown on a silicon substrate with a carbon content of 0.2%, 0.5%, and 1.2%, respectively. The carbon concentrations of these pseudomorphic layers were obtained according to Vegard's law by x-ray diffraction measurements.[8] This method can only be used for strained layers. The full width at half maximum (FWHM) of the local vibrational mode of carbon in monocrystalline silicon is 5.9 cm^{-1} at room temperature. There have been various attempts to determine the concentration of substitutional carbon from the the strength of this local vibrational modes, but all these methods have to be treated with care.[10] A rather big

problem as to determining the substitutional carbon concentration arises for strained alloy layers, because the FWHM increases already at a carbon concentration of 0.2% to more than 11 cm^{-1} compared to the 5.9 cm^{-1} in monocrystalline silicon. With rising carbon concentration and, therefore, increasing strain, the FWHM increases up to more than 16 cm^{-1} for samples with carbon concentrations of more than 1%. To determine the carbon concentration from the absorbance one also has to know the thickness of the layers. The thickness of the layers in Fig. 5 as determined from x-ray measurements was about 540 nm (0.2%), 350 nm (0.5%), and 100 nm (1.2%), respectively, with an error of about 5%. For more exact values of the thickness one has to use a transmission electron microscope. Thus, the determination of the carbon concentration from absorption measurements is rather inaccurate. For better comparison the Raman, IR absorption, and x-ray measurements were performed on the same sample spots.

As discussed above for the Raman measurements, we also observe in the IR absorption spectrum a definite satellite peak on the high-energy side of the substitutional carbon local vibrational mode and possibly weak indications on the low-energy side. The strength of the satellite peaks depends to some extent on the position on the sample.

All the MBE-grown samples have a boron background doping of the layer below 10^{16} cm^{-3}. Additionally, boron atoms gather at the interface between the Si substrate and the $Si_{1-x}C_x$ alloy with a surface density of about 10^{12} cm^{-2}. The maximum of the high-energy satellite peak at 625 cm^{-1} (Fig. 5) lies close the vibrational mode of the substitutional boron isotope with mass number 11, which appears at 623 cm^{-1} in monocrystalline silicon. But the attribution to boron can be definitely excluded for the following reasons: (i) The boron peak should not be observed in a layer only 300 nm thick. (ii) Boron has two isotopes with mass numbers 10 and 11, which have a natural abundance of 20% and 80%, respectively. Thus one should observe at least a weak peak at about 645 cm^{-1}, where the isotope with a mass of 10 shows its vibration in monocrystalline silicon. Our signal-to-noise ratio is good enough to exclude a peak due to ^{10}B. (iii) It has been shown that most of the interfacial boron is not electrically active,[20] indicating that the interfacial boron does not occupy substitutional lattice positions. In sum, the observed strong satellite peak must have a different origin and we attribute it to the third-nearest-neighbor carbon pair.

IV. DISCUSSION

The results of the previous section show that both Raman spectroscopy and infrared absorption confirm the satellite structure in the local vibrational modes of carbon in $Si_{1-x}C_x$ alloys that was predicted by the lattice-dynamical calculation. However, the experiments only detect the peak associated with the third-nearest-neighbor C-C pair. By comparing the theoretical and measured spectra, we can deduce that this shows an enhanced probability of third-nearest-neighbor pairs in the samples. Although a detailed understanding of the MBE growth process is difficult to obtain, such an enhancement is conceivable in view of the energy gain for this configuration of the carbon atoms.

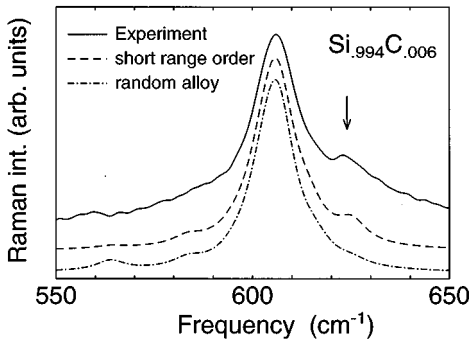

FIG. 6. First-order Raman spectrum of Si-C vibrations in a pseudomorphic $Si_{0.994}C_{0.006}$ layer on Si(001). The experimental spectrum (full line) shown in the upper curve was obtained by subtracting the signals of the uncovered substrate from the signal measured for the heterostructure (epilayer + substrate) as explained in the main text. The arrow indicates the satellite peak at 625 cm^{-1} arising from 3nn C-C pairs. Calculated Raman spectra are shown for a random $Si_{0.994}C_{0.006}$ alloy (dash-dotted line) as well as for an alloy where the occurrence of bound 3nn C-C pairs was enhanced by a factor of 4 with respect to the random occupation while the occurrence of unbound 2nn pairs was reduced by a factor of 4 (dashed line).

The continuous line in Fig. 6 shows a typical measured Raman spectrum for a $Si_{0.994}C_{0.006}$ layer, obtained as described in Sec. II C. The measurements clearly show a satellite peak at the high-frequency side of the spectrum at about 625 cm^{-1}. This peak was observed in a series of samples with carbon concentrations ranging from 0.001 to $x=0.012$. The main Si-C peak of the $Si_{0.994}C_{0.006}$ layer has its maximum at 605 cm^{-1} and a FWHM of 12 cm^{-1}.

The anharmonic Keating model predicts the main Si-C peak at 612 cm^{-1}. Considering the simplicity of the model, this is in remarkably good agreement with the experimental value, showing the validity of the derived scaling for the force constants. For a better comparison we have shifted the calculated spectra by 7 cm^{-1} to lower frequencies. All spectra used a Lorentzian broadening of $\Gamma=12$ cm^{-1} taken from the measured width of the main Si-C peak. The lower curve in Fig. 6 is the calculated spectrum of the random $Si_{0.994}C_{0.006}$ alloy, obtained as a correctly weighted superposition of the spectra for C-C pairs as described in Sec. II C. This spectrum shows only a very slight shoulder above the the main Si-C signal. (Note that the broadening is bigger than in Fig. 2.) Thus, the formation of an experimentally well-resolved satellite at the frequency predicted for the 3nn C-C pair can only be explained when an increased concentration of these pairs is assumed.

Given the interaction function for the C-C pairs, it is conceivable that diffusion during sample growth influences the arrangement of the carbon impurities away from a purely random occupation. To reduce the total energy, more 3nn pairs should be produced while at the same time the energetically strongly unfavorable 2nn should be avoided. This can be visualized as randomly deposited 2nn pairs that quickly separate to a 3nn position, although the true growth process is no doubt considerably more complicated. To model such an effect in a rough way, a second spectrum was

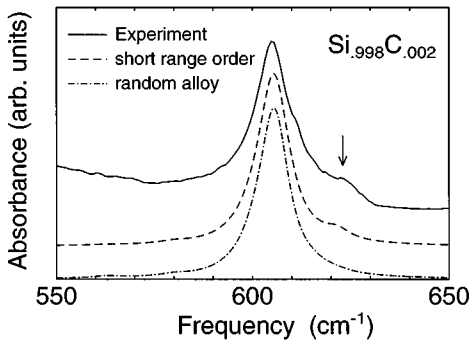

FIG. 7. Infrared absorption in the frequency range of Si-C vibrations for a pseudomorphic $Si_{0.998}C_{0.002}$ layer on Si(001) (full line). As for the Raman spectra shown in Fig. 6, the dash-dotted line shows the theoretical spectrum for a purely random occupation and the dashed line shows the spectrum when the occurrence of third- and second-nearest-neighbor pairs is enhanced (respectively, reduced) by a factor of 4. The arrow indicates the satellite peak due to 3nn C-C pairs.

calculated with the number of 3nn pairs increased by a factor of 4 and that of the 2nn pairs reduced by the same factor. The calculated Raman spectrum for this partially ordered alloy (Fig. 6) now shows a 3nn satellite peak comparable to that seen in the measured spectrum.

A similar analysis for the infrared spectra confirms this procedure. In Fig. 7 a typical measured spectrum for a $Si_{0.998}C_{0.002}$ layer is shown. Again, the experimentally observed satellite peak near 625 cm^{-1} cannot be reproduced by calculations for the purely random alloy. Using the same enhancement and reduction factors for the 3nn and 2nn peaks as before, a similar agreement between theory and experiment is obtained.

Overall, we are conscious that this interpretation of the Raman and infrared spectra is far from quantitative. Nevertheless, it seems clear that the calculated attractive C-C pair interaction energy is confirmed by these results, demonstrating that the third-nearest-neighbor configuration is substantially enhanced in a MBE-grown dilute $Si_{1-x}C_x$ alloy. For a $Si_{0.994}C_{0.006}$ alloy and an enhancement by a factor of 4, already every fourth C atom is a member of such a 3nn pair, whereas this would be only about 1 in 15 for a purely random distribution. Note that if the crystal were to contain *only* third-nearest-neighbor pairs, the main Si-C peak would still be twice as large as the satellite due to the unshifted subpeaks seen in Fig 3. Thus, the admittedly rather small satellite peak seen in the experiment indicates a distinct qualitative difference relative to the random alloy.

V. SUMMARY

In this paper, we have combined theory and experiment to study the local carbon vibrational modes of substitutional $Si_{1-x}C_x$ alloys. Due to the large difference in mass, the surrounding Si atoms participate only to a very small extent in these vibrations. Nevertheless, the calculations predict a sizable interaction between carbon atoms even when these are further apart than second-nearest neighbors. This is not the direct interaction of the vibrations on the two carbon sites. Instead, the strain field around each carbon atom distorts the environment around the second one. Because of the large size difference between Si and C atoms, these strain effects are much larger than in related compounds such as Si-Ge alloys. A good description, therefore, is to consider isolated carbon impurities, vibrating in an unsymmetric local environment.

Within this picture, a direct connection between the local vibrational modes and the pair-interaction energy of two substitutional carbon impurities emerges. The pair interaction is due to elastic effects, whereby a bound configuration (notably the third-nearest-neighbor arrangement) arises when the local geometry permits a better relaxation of the Si-C bonds towards their short equilibrium length. These bonds are comparatively stiff, leading to vibrational modes that lie at higher frequencies compared to the mode of an isolated C impurity. Similarly, an energetically unfavorable arrangement is associated with longer and softer Si-C bonds and a reduced vibrational frequency.

Careful measurements using Raman and infrared spectroscopy on MBE-grown dilute $Si_{1-x}C_x$ samples could detect a satellite peak above the main C impurity peak at the frequency predicted for the third-nearest-neighbor C-C pair. The experimental spectra were compared to theoretical results for alloys of the same composition, whereby a random occupation of each site according to the stoichiometry was assumed. Interestingly, these calculated spectra show a much smaller amplitude for the satellite peak than was found in the experiment. Adequate agreement between theory and experiment could only be reached if the probability for finding third-nearest-neighbor C-C pairs is enhanced by a factor in the vicinity of 4 relative to the purely random alloy. This leads to the conclusion that the carbon atoms in the samples show a distinct short-range order with a high percentage of 3nn C-C pairs. Overall, we obtain a confirmation of the calculated pair-interaction curve, which predicts a sizable energy gain at this distance.

[1] K. Eberl, S. S. Iyer, S. Zollner, J. C. Tsang, and F. K. LeGoues, Appl. Phys. Lett. **60**, 3033 (1992).
[2] A. R. Powell, K. Eberl, B. A. Ek, and S. S. Iyer, J. Cryst. Growth **127**, 425 (1993).
[3] J. W. Strane, H. J. Stein, S. R. Lee, S. T. Picraux, J. K. Watanabe, and J. W. Mayer, J. Appl. Phys. **76**, 3656 (1994).
[4] S. C. Jain, H. J. Osten, B. Dietrich, and H. Rücker, Semicond. Sci. Technol. **10**, 1289 (1995).
[5] J. C. Tsang, K. Eberl, S. Zollner, and S. S. Iyer, Appl. Phys. Lett. **61**, 961 (1992).
[6] J. Menendez, P. Gopalan, G. S. Spencer, N. Cave, and J. Strane, Appl. Phys. Lett. **66**, 1160 (1995).
[7] B. Dietrich, H. J. Osten, H. Rücker, M. Methfessel, and P. Zaumseil, Phys. Rev. B **49**, 17 185 (1994).
[8] H. J. Osten, E. Bugiel, and P. Zaumseil, Appl. Phys. Lett. **64**, 3440 (1994).

[9] D. Endisch, H. J. Osten, P. Zaumseil, and M. Zinke-Allmany, Nucl. Instrum. Methods Phys. Res. Sect. B **100**, 125 (1995).
[10] G. Davies and R. C. Newman, in *Handbook of Semiconductors*, edited by T. S. Moss (Elsevier Science, New York, 1994), Vol. 3.
[11] J. Tersoff, Phys. Rev. Lett. **64**, 1757 (1990).
[12] H. Rücker, M. Methfessel, E. Bugiel, and H. J. Osten, Phys. Rev. Lett. **72**, 3578 (1994).
[13] H. Rücker and M. Methfessel, Phys. Rev. B **52**, 11 059 (1995).
[14] P. N. Keating, Phys. Rev. **145**, 637 (1966).
[15] S. Baroni, S. de Gironcoli, and P. Giannozzi, Phys. Rev. Lett. **65**, 84 (1990).
[16] M. Born and K. Huang, *Dynamical Theory of Crystal Lattices* (Clarendon Press, Oxford, 1988).
[17] R. M. Martin, Phys. Rev. B **1**, 4005 (1970).
[18] *Physics of Group IV Elements and III-V Compounds*, edited by O. Madelung *et al.*, Landolt-Börnstein, New Series, Group III, Vol 17, Pt. a (Springer-Verlag, Berlin, 1982).
[19] P. A. Temple and C. A. Hathaway, Phys. Rev. B **7**, 3685 (1973).
[20] P. Garworzewski, D. Krüger, R. Kurps, H. Rücker, and H. P. Zeindl, J. Appl. Phys. **75**, 7869 (1994).